IKR Publishers

IKR Journal of Engineering and Technology (IKRJET)
Journal homepage: https://ikrpublishers.com/ikrjet/
Volume-2, Issue-4 (July-August) 2026

OPEN ACCESS
ISSN: 3107-7331 (Online)

From Mineralogy to Process Design: The Role of Particle Size Distribution on Nickel Extraction Kinetics and Hydrometallurgical Route Selection in a Limonitic Laterite

Antonio Clareti Pereira, PhD*
PhD in Chemical Engineering University of São Paulo (USP) Belo Horizonte, Minas Gerais, Brazil

DOI:*10.5281/zenodo.21209619*

ARTICLE INFO

Article history:
Received : 23-06-2026
Accepted : 30-06-2026
Available online : 05-07-2026

Citation: Pereira, A. C. (2026). From Mineralogy to Process Design: The Role of Particle Size Distribution on Nickel Extraction Kinetics and Hydrometallurgical Route Selection in a Limonitic Laterite. *IKR Journal of Engineering and Technology (IKRJET), 2*(4), 1-17.

ABSTRACT **Original Research Article**

The mineralogical distribution of nickel within lateritic ores plays a fundamental role in leaching performance and process selection. This study investigated the influence of particle size on mineralogy, leaching kinetics, and nickel extraction using a limonitic nickel laterite from Northeastern Brazil. The ore was separated into coarse (>100#) and fine (<100#) fractions and characterized by chemical and mineralogical analyses. The coarse fraction was enriched in serpentine, vermiculite, and a poorly crystalline Fe–Si phase, whereas the fine fraction was dominated by iron oxyhydroxides (goethite–limonite). Atmospheric sulfuric acid leaching tests were performed at 95–99°C for 7 h using 600 g of ore, 600 g of H_2SO_4, and 1800 g of water. Process variables, including pH, redox potential, free acidity, liquor density, and elemental concentrations, were monitored throughout the experiments. Nickel extraction reached approximately 95% in both fractions; however, marked differences in dissolution kinetics were observed. The coarse fraction exhibited faster initial nickel extraction due to the rapid dissolution of nickel-bearing phyllosilicates and Mg-rich phases, while the fine fraction displayed slower kinetics associated with the progressive dissolution of goethitic iron phases. Correlations between Ni, Fe, and Mg extraction demonstrated the strong mineralogical control of metal release. Kinetic modeling indicated distinct rate-controlling mechanisms between granulometric fractions. The results suggest that nickel associated with phyllosilicates and poorly crystalline Fe–Si phases can be efficiently recovered by atmospheric leaching, whereas nickel hosted in iron oxyhydroxides may be more suitable for high-pressure acid leaching (HPAL). A geometallurgical processing strategy based on particle-size classification is proposed to optimize route selection and improve overall process efficiency.

Keywords: Nickel Laterite, Atmospheric Leaching, Leaching Kinetics, Geometallurgy, Mineralogical Partitioning, Process Route Selection.

Highlights

- Particle size strongly controls the mineralogical distribution of nickel-bearing phases in lateritic ores.
- Coarse fractions enriched in phyllosilicates exhibit faster nickel dissolution than fine goethitic fractions under atmospheric leaching conditions.
- Nickel extraction kinetics are governed by distinct mineralogical hosts, resulting in different rate-controlling mechanisms.
- Particle-size classification provides a geometallurgical basis for directing coarse fractions to atmospheric leaching and fine fractions to HPAL processing.

Graphical Abstract

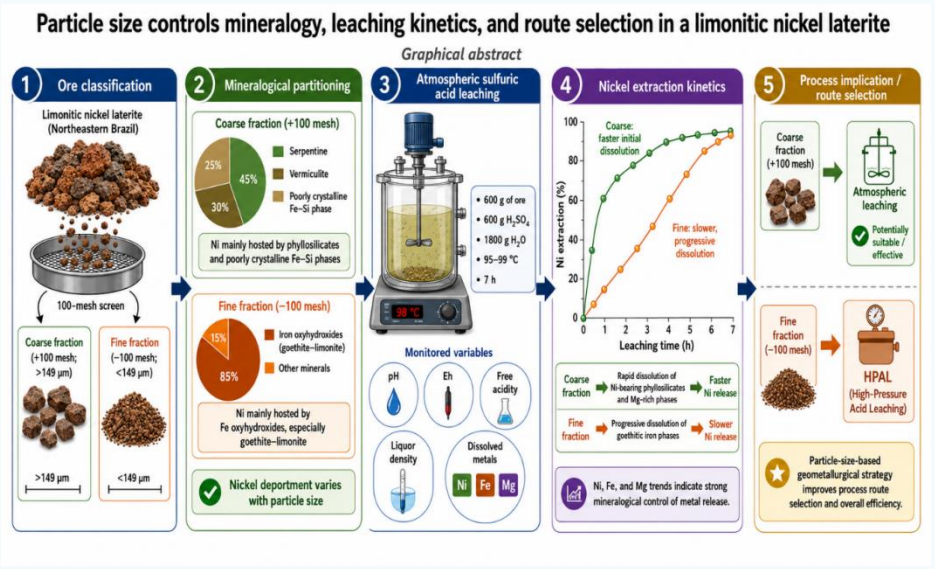

*Corresponding author: Antonio Clareti Pereira, PhD
PhD in Chemical Engineering University of São Paulo (USP) Belo Horizonte, Minas Gerais, Brazil

Introduction

Nickel has become one of the most strategically important metals for the global energy transition because of its extensive use in rechargeable batteries, electric vehicles, and large-scale energy storage systems. The rapid growth of battery manufacturing has substantially increased the demand for Class I nickel and intensified the search for new resources and more efficient extraction technologies. Lateritic deposits account for the majority of global nickel resources and are expected to play an increasingly important role in meeting future demand. At the same time, environmental constraints, resource depletion, and economic pressures are driving the mining industry toward the exploitation of lower-grade and more complex laterite ores (Pell et al., 2021; Golroudbary et al., 2023; Soh Tamehe et al., 2024).

Hydrometallurgical processing has become the dominant route for the treatment of nickel laterites. High-pressure acid leaching (HPAL) is widely recognized as the most effective technology for limonitic ores because it can achieve high nickel and cobalt recoveries. However, HPAL is associated with high capital investment, elevated acid consumption, complex autoclave operation, and significant iron dissolution, which increases downstream neutralization and residue management requirements (Çoban & Baş, 2024; Gharaei et al., 2024; Dickson et al., 2025; Bana et al., 2025; Surya et al., 2026). As a result, alternative processing routes continue to attract attention. Atmospheric sulfuric acid leaching has emerged as a promising option for selected lateritic feedstocks because of its lower capital intensity, operational simplicity, and potential for integration into flexible process flowsheets. Recent studies have reported encouraging nickel and cobalt recoveries under atmospheric conditions through the optimization of variables such as acid dosage, temperature, residence time, and redox conditions (Hosseini Nasab et al., 2020; Astuti et al., 2024; Prameswara et al., 2024; Prasetya et al., 2025; Ribeiro et al., 2025).

The response of lateritic ores to hydrometallurgical treatment is strongly controlled by mineralogy. Nickel may occur in iron oxyhydroxides such as goethite and limonite, in phyllosilicates including serpentine and vermiculite, or in poorly crystalline ferruginous silicate phases. These mineral hosts exhibit varying reactivities toward acidic solutions, thereby influencing extraction kinetics, acid consumption, metal selectivity, and overall process performance. Consequently, mineralogical characterization has become an essential component of modern geometallurgical programs aimed at linking ore properties with metallurgical behavior (Dehaine et al., 2021; Butcher et al., 2023). Previous investigations have demonstrated that significant variations in nickel recovery can occur even among ores with similar bulk chemical compositions because of differences in mineral assemblages, textural relationships, and metal deportment (Dybowska et al., 2022; Jeong et al., 2025; Araujo et al., 2026).

Despite these advances, the relationship between particle size, mineralogical nickel deportment, and metallurgical performance remains insufficiently understood. Most studies of nickel laterite leaching have focused on operational variables such as temperature, acid concentration, pressure, and residence time, while treating the ore as a chemically and mineralogically homogeneous material (Top et al., 2020; Li et al., 2020; Yunita & Mubarok, 2021; Komnitsas et al., 2026; Ni'mah et al., 2026). Although the influence of mineralogy on extraction is widely recognized, comparatively few investigations have examined how nickel-bearing phases are distributed across different particle-size fractions and how

this distribution affects dissolution behavior. Even fewer studies have integrated mineralogical partitioning, extraction kinetics, and metallurgical response into a unified framework that explains why different size fractions behave differently during leaching. Consequently, the mechanistic links between granulometric classification, mineralogical nickel hosts, and hydrometallurgical performance remain poorly established. Furthermore, the potential use of particle-size-dependent mineralogical information as a criterion for process route selection has received limited attention in the nickel laterite literature.

This study investigates the influence of particle-size classification on mineralogical partitioning, nickel deportment, and sulfuric acid leaching behavior in a limonitic nickel laterite from Northeastern Brazil. The working hypothesis is that nickel is unevenly distributed among phyllosilicates, poorly crystalline Fe–Si phases, and iron oxyhydroxides, and that the relative abundance of these hosts varies with particle size, thereby affecting dissolution kinetics, acid response, and hydrometallurgical route selection. By combining mineralogical characterization, atmospheric leaching tests, and kinetic modeling, the study provides a geometallurgical framework linking particle-size fractionation to processing performance.

Materials and Methods

Ore Sampling

A bulk sample of a limonitic nickel laterite from Northeastern Brazil was collected and homogenized for mineralogical and metallurgical characterization. The deposit is representative of tropical lateritic weathering systems developed under intense chemical weathering conditions (Dybowska et al., 2022; Domènech et al., 2022; Soh Tamehe et al., 2024).

Representative subsamples were prepared by successive crushing, homogenization, and riffle splitting procedures. Chemical analyses were performed to determine major and minor components, as presented in Table 1.

Table 1. Chemical composition of the lateritic nickel ore used in this study.

Compound	Content (wt.%)
Fe_2O_3	48.72
SiO_2	24.76
H_2O (bound)	11.58
MgO	6.26
Al_2O_3	3.62
Cr_2O_3	2.84
NiO	1.13
MnO	0.82
CaO	0.13
CoO	0.08
ZnO	0.04
CuO	0.0124
FeO	0.00
H_2O (free)	0.00
Total	100.00

Source: Authors, based on laboratory chemical analyses.

The ore is characterized by a high Fe_2O_3 content (48.72 wt.%) and significant SiO_2 content (24.76 wt.%), indicating a ferruginous-siliceous lateritic composition typical of limonitic weathering profiles. The presence of 11.58 wt.% structurally bound water suggests a substantial proportion of hydrated iron oxyhydroxides, particularly goethite and limonite. Magnesium oxide accounts for 6.26 wt.% of the ore, indicating the occurrence of Mg-bearing phyllosilicates such as serpentine and vermiculite. Nickel and cobalt occur at 1.13 wt.% NiO and 0.08 wt.% CoO, respectively, confirming the economic relevance of the deposit. The elevated iron content, combined with moderate magnesium levels, suggests a transitional mineralogical assemblage in which nickel may be distributed among iron oxyhydroxides, phyllosilicates, and poorly crystalline Fe–Si phases. This compositional complexity provides an appropriate framework for investigating the influence of particle size on mineralogical partitioning and leaching behavior.

Particle Size Separation

The homogenized sample was screened at 100 mesh (149 µm), generating two particle-size fractions:

- Coarse fraction (>100#; >149 µm)
- Fine fraction (<100#; <149 µm)

This approach follows geometallurgical principles, in which particle-size fractions may exhibit different mineralogical characteristics and, consequently, different processing behaviors (Dehaine et al., 2021; Butcher et al., 2023).

To investigate the influence of particle size on mineralogical distribution and metallurgical performance, the bulk ore

sample was separated into two granulometric fractions using a 100-mesh (149 µm) screen. This classification produced a coarse fraction enriched in larger particles and a fine fraction enriched in iron-rich fines. The selected cut size approximates the transition between coarse liberated particles and fine limonitic particles commonly observed in nickel laterites. This size also provided sufficient mass in both fractions for mineralogical characterization and replicated leaching experiments. The particle-size fractions evaluated in this study are summarized in Table 2.

Table 2. Particle-size fractions evaluated in the study.

Fraction	Tyler Mesh	Particle Size Range	Description	Purpose
Coarse Fraction	+100#	>149 µm	Material retained on the 100-mesh screen	Mineralogical characterization and atmospheric leaching
Fine Fraction	−100#	<149 µm	Material passing the 100-mesh screen	Mineralogical characterization and atmospheric leaching

Source: Authors.

The particle-size classification provided the basis for assessing the relationship between granulometry, mineralogical partitioning, and nickel extraction behavior. Previous geometallurgical studies have shown that different particle-size fractions may exhibit distinct mineral assemblages and metal deportment patterns, which can significantly affect leaching kinetics and process performance (Dehaine et al., 2021; Butcher et al., 2023). Consequently, both fractions were independently characterized and tested to determine whether particle-size-dependent mineralogical variations could influence the selection of hydrometallurgical routes.

Mineralogical Characterization

Mineralogical characterization was performed using optical microscopy, X-ray diffraction (XRD), scanning electron microscopy coupled with energy-dispersive spectroscopy (SEM–EDS), and automated mineralogical analysis.

Optical microscopy was performed on polished sections under reflected lightto identify mineral phases and textural relationships.

XRD analyses were performed using Cu Kα radiation over a 2θ range suitable for identifying crystalline phases.

SEM–EDS was employed to evaluate particle textures, phase associations, and elemental distributions.

Automated mineralogical characterization was carried out using MLA/QEMSCAN methodologies to quantify modal mineralogy and nickel deportment.

These techniques have been widely applied in geometallurgical investigations of lateritic ores because they provide complementary information regarding mineral abundance, textural relationships, and metal deportment (Dehaine et al., 2021; Butcher et al., 2023).

Detailed mineralogical characterization identified nickel-bearing phases and their size distribution. Results showed significant partitioning: the coarse fraction was enriched in phyllosilicates and ferruginous silicates, whereas the fine fraction was enriched in iron oxyhydroxides. The modal mineralogies are in Table 3.

Table 3. Modal mineralogical composition of coarse and fine fractions.

Mineral Phase	Coarse Fraction (>100#) (%)	Fine Fraction (<100#) (%)
Iron oxyhydroxides (goethite–limonite)	27.66	69.43
Poorly crystalline Fe–Si phase	23.20	14.45
Vermiculite–chlorite	13.94	3.82
Serpentine	4.88	1.18
Chromite	10.38	3.18
Quartz–chalcedony	9.25	1.39
Other minerals	10.69	6.55
Total	100.00	100.00

Source: Authors, based on mineralogical characterization results.

The results demonstrate a pronounced enrichment of iron oxyhydroxides in the fine fraction, where goethite–limonite accounts for approximately 69% of the mineral assemblage. In contrast, the coarse fraction contains substantially higher proportions of vermiculite–chlorite, serpentine, chromite, and poorly crystalline Fe–Si phases. These observations indicate that particle-size classification effectively separates mineralogical domains with distinct nickel hosts.

Atmospheric Leaching Tests

Atmospheric sulfuric acid leaching experiments were conducted under controlled laboratory conditions. For each

test, 600 g of ore were mixed with 600 g of sulfuric acid and 1800 g of water, resulting in a total slurry mass of 3000 g.

The experiments were performed at temperatures ranging from 95 to 99 °C for 7 h. During leaching, periodic samples were collected to monitor pH, redox potential (Eh), free acidity, liquor density, and dissolved metal concentrations. Similar experimental conditions have been reported in previous investigations of atmospheric leaching of nickel laterites (Hosseini Nasab et al., 2020; Santos et al., 2021; Astuti et al., 2024; Prameswara et al., 2024; Prasetya et al., 2025).

Acidity control and interpretation followed methodologies commonly applied in hydrometallurgical systems involving sulfuric acid leaching (Pereira et al., 2025; Pereira, 2026a; Pereira, 2026b).

Atmospheric sulfuric acid leaching experiments tested how particle size and mineralogy affect nickel extraction under controlled lab conditions. Using a fixed acid-to-ore ratio, the experiments monitored temperature, pH, redox potential, free acidity, slurry traits, and solution chemistry. Key conditions are summarized in Table 4.

Table 4. Operational parameters employed during atmospheric sulfuric acid leaching experiments.

Parameter	Value	Unit
Ore mass	600	g
Sulfuric acid mass	600	g
Water mass	1800	g
Initial slurry mass	3000	g
Solid concentration	20.0	wt.%
Leaching temperature	95–99	°C
Leaching time	7	h
Atmospheric pressure	1	atm
Initial pH	-0.52	—
Final pH	0.15	—
Initial Eh	1163	mV
Final Eh	1028	mV
Initial free acidity	3.08	g L^{-1} H_2SO_4
Final free acidity	2.12	g L^{-1} H_2SO_4
Sampling times	0.5, 1, 2, 4, 5, 6, 7	h
Final residue mass (dry basis)	258.58	g
Final pregnant leach solution volume	991.07	mL
Washing water volume	1922.81	mL

Source: Authors.

The selected operating conditions were designed to promote substantial nickel dissolution while maintaining temperatures achievable under atmospheric pressure. Continuous monitoring of pH, Eh, and free acidity provided information regarding acid consumption and reaction progress throughout the leaching period. Periodic sampling enabled the construction of extraction curves for Ni, Co, Fe, Mg, and Mn, which were subsequently used for kinetic modeling and evaluation of the mechanisms controlling metal dissolution. The combination of controlled operating conditions and detailed monitoring yielded a comprehensive dataset to assess the relationships among mineralogy, particle size, and leaching performance.

All leaching experiments were performed in quadruplicate.

Quality Assurance and Data Treatment

All chemical analyses were performed using certified analytical procedures routinely applied by the laboratory for lateritic ores, leach liquors, wash waters, and solid residues.

The experimental program comprised four leaching tests for each particle-size fraction, all conducted under the same initial acid dosage, solid/liquid ratio, temperature range, and total leaching time. Therefore, the tests were treated as repeated operating responses under fixed leaching conditions, and the observed variability was interpreted mainly in terms of particle-size fraction, mineralogical heterogeneity, nickel deportment, sampling effects, and mass-balance uncertainty, rather than changes in acid addition.

For each test, metal extraction was calculated from the distribution of elements between the liquid and solid phases. The solution phase included both the pregnant leach solution and the corresponding wash liquor, while the solid phase corresponded to the washed residue. Mass balance closure was evaluated using the distributions of Ni, Fe, Mg, Mn, and the principal gangue-forming elements between solution and residue streams. Results presenting mass balance closures between 95 and 105% were considered acceptable for subsequent interpretation.

Magnesium-corrected extraction values were used to reduce the effect of sampling, dilution, and solid–liquid separation uncertainties. Final extraction values obtained after 420 min were statistically evaluated using the mean, standard deviation, and coefficient of variation. These parameters were used to assess the dispersion of metallurgical response across the investigated operating window.

Analytical uncertainty was assessed using laboratory quality-control procedures and, when available, replicate analytical measurements. Kinetic model performance was evaluated using the coefficient of determination (R^2). Models with higher R^2 values were considered to better represent the experimental nickel extraction curves, provided that the fitted trend was consistent with the expected leaching mechanism.

Kinetic Analysis

The influence of mineralogy on nickel extraction kinetics was evaluated using classical heterogeneous reaction models. The objective was to identify the rate-controlling mechanism governing dissolution in each granulometric fraction.

The Shrinking Core Model (SCM) was applied considering two possible controlling mechanisms:

Chemical Reaction Control

$$1 - (1 - X)^{\frac{1}{3}} = kt$$

Where:

X is the fractional conversion;
k is the apparent kinetic constant;
t is the leaching time.

Product Layer Diffusion Control

$$1 - 3(1 - X)^{\frac{2}{3}} + 2(1 - X) = kt$$

To complement the analysis, empirical kinetic models frequently employed in hydrometallurgical systems were also evaluated.

Pseudo-First-Order Model

$$\ln(1 - X) = -kt$$

Pseudo-Second-Order Model

$$\frac{t}{X} = \frac{1}{kX_e^2} + \frac{t}{X_e}$$

Where:

Xe is the equilibrium conversion;
k is the apparent rate constant.

The applicability of each model was assessed through linear regression analysis. The coefficient of determination (R^2) was used to compare model performance and identify the dominant dissolution mechanism. Similar approaches have been successfully applied in nickel laterite leaching studies (Garces-Granda et al., 2020; Li et al., 2020; He et al., 2022a; He et al., 2022b; Borda & Torres, 2023; Alif et al., 2025; Shayakhmetova et al., 2025; Tyassena et al., 2026).

Results

Mineralogical Partitioning

Mineralogical characterization revealed significant differences between the coarse (>100#) and fine (<100#) fractions. The particle-size classification resulted in a clear redistribution of the principal mineral phases within the ore. Iron oxyhydroxides were concentrated in the fine fraction, whereas phyllosilicates and poorly crystalline Fe–Si phases were more abundant in the coarse fraction.

These results indicate that granulometric classification produced distinct mineralogical domains, despite both fractions originating from the same ore sample. Similar mineralogical partitioning has been reported in tropical lateritic profiles, where weathering processes generate heterogeneous distributions of iron-rich and silicate-rich phases across particle-size classes (Dybowska et al., 2022; Jeong et al., 2025; Kang et al., 2026).

The modal mineralogical compositions obtained for the coarse and fine fractions are summarized in Figure 1.

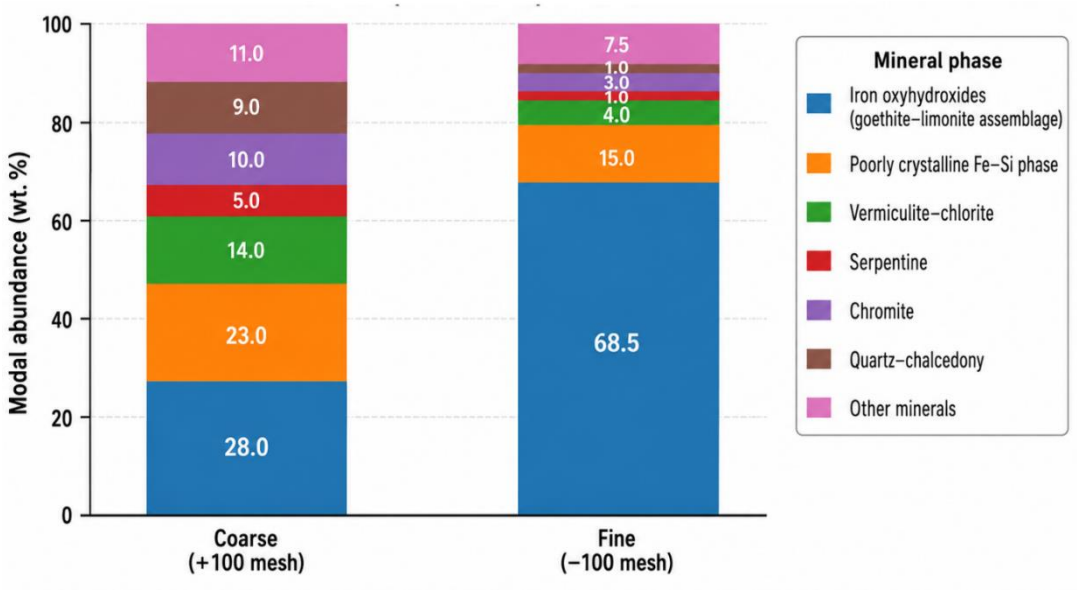

Figure 1. Modal mineralogical distribution of coarse (>100#) and fine (<100#) fractions.
Source: Authors.

The fine fraction exhibited a substantially higher proportion of iron oxyhydroxides, whereas the coarse fraction contained larger amounts of serpentine, vermiculite–chlorite, and poorly crystalline Fe–Si phases. These differences suggest that nickel deportment may vary significantly between particle-size fractions.

Distribution of Nickel-Bearing Phases

Nickel deportment analysis demonstrated that the metal was distributed among several mineral hosts. The principal nickel-bearing phases identified were goethite–limonite, poorly crystalline Fe–Si phases, serpentine, and vermiculite–chlorite.

The distribution of nickel among these phases differed markedly between the coarse and fine fractions. Nickel associated with phyllosilicates was more abundant in the coarse fraction, whereas nickel associated with iron oxyhydroxides was concentrated in the fine fraction. Similar nickel deportment patterns have been reported in lateritic ores where weathering intensity controls the redistribution of nickel between silicate and ferruginous mineral hosts (Hariyanto et al., 2023; Jeong et al., 2025; Araujo et al., 2026).

Figure 2 presents the estimated distribution of nickel among the principal mineral hosts identified in the ore.

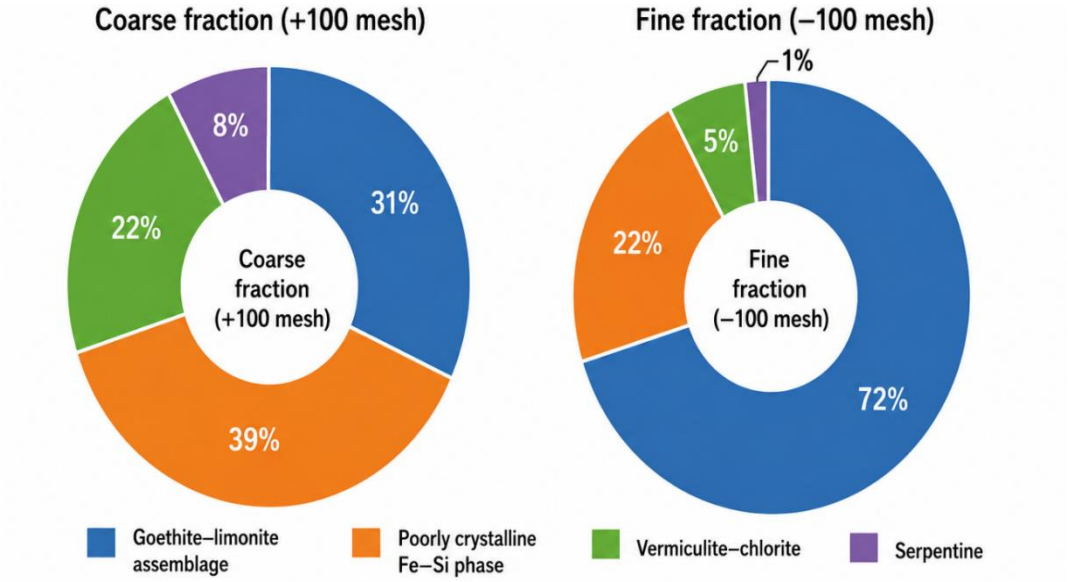

Figure 2. Distribution of nickel among goethite–limonite, poorly crystalline Fe–Si phases, serpentine, and vermiculite–chlorite.
Source: Authors.

The results demonstrate that nickel was not uniformly distributed throughout the ore. Instead, its deportment was strongly linked to mineralogical composition, providing an important basis for interpreting the extraction behavior observed during leaching.

Atmospheric Leaching Performance

Atmospheric sulfuric acid leaching resulted in high final nickel extraction for both particle-size fractions after 420 min of reaction. Under the fixed initial acid dosage evaluated in this study, magnesium-corrected nickel extraction ranged from 85.3 to 103.1% for the coarse fraction and from 85.3 to 98.6% for the fine fraction. Because the leaching tests were conducted under equivalent operating conditions, including acid dosage, solid/liquid ratio, temperature range, and total leaching time, the observed differences in extraction behavior are attributed mainly to particle-size fraction, mineralogical heterogeneity, nickel deportment, sampling effects, and mass-balance variability, rather than to changes in acid addition.

Values slightly above 100% are interpreted as the result of cumulative analytical uncertainty, sampling effects, and mass-balance variability associated with the correction procedure. The extraction levels obtained after prolonged leaching are consistent with those reported for atmospheric leaching of limonitic and transitional nickel laterites under comparable sulfuric acid leaching conditions (Hosseini Nasab et al., 2020; Santos et al., 2021; Astuti et al., 2024; Prasetya et al., 2025; Ribeiro et al., 2025).

The high final recoveries indicate that, when sufficient residence time is provided, both granulometric fractions are capable of reaching elevated nickel extraction under atmospheric sulfuric acid leaching conditions. Therefore, the final extraction values alone do not fully express the effect of particle size. Although both fractions approached high nickel recovery after 420 min, the kinetic behavior showed that the coarse fraction reached elevated extraction levels earlier, whereas the fine fraction required longer reaction time to attain comparable recovery.

This behavior indicates that particle size and mineralogical deportment exerted a stronger influence on the rate of nickel dissolution than on the ultimate nickel extraction achieved after prolonged leaching. In practical terms, the granulometric effect was expressed mainly through leaching kinetics and residence-time requirements. The coarse fraction exhibited faster initial dissolution, while the fine fraction showed a slower approach to high recovery, consistent with differences in nickel-bearing mineral hosts, mineral exposure, and reactivity under atmospheric sulfuric acid leaching conditions.

Overall, these results suggest that, under fixed acid-dosage conditions, particle-size fraction affects primarily the leaching rate rather than the final nickel extraction after extended reaction time. This distinction is important for process interpretation, because similar final recoveries may mask relevant differences in dissolution kinetics, acid accessibility, and residence-time demand.

Nickel Extraction Kinetics

The nickel extraction curves for the coarse and fine fractions in Figure 3 show rapid initial dissolution followed by a slowdown. The coarse fraction initially had a higher extraction, but the differences diminished over time, with both approaching similar recoveries after 6–7 hours.

Similar kinetic behavior occurs in nickel laterite leaching, where mineralogical differences affect initial dissolution but have less impact on overall recovery (Garces-Granda et al., 2020; He et al., 2022b; Alif et al., 2025; Kang et al., 2026).

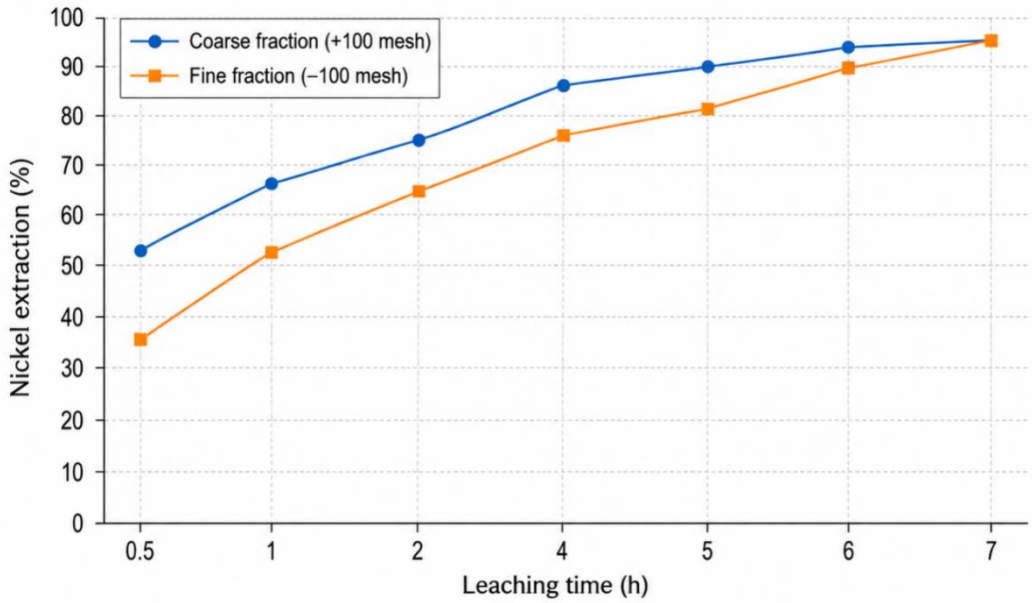

Figure 3. Nickel extraction kinetics for coarse and fine fractions during atmospheric sulfuric acid leaching.
Source: Authors.

The higher initial extraction rate observed for the coarse fraction indicates a greater availability of readily leachable nickel-bearing phases during the early stages of the process.

Dissolution of Major Elements

The dissolution behavior of magnesium, nickel, and iron differed significantly during leaching. Magnesium exhibited

the highest dissolution rate and reached near-complete extraction early in the process. Nickel extraction followed a similar trend during the initial stages of leaching, whereas iron dissolution proceeded more gradually throughout the experiment.

The observed behavior is consistent with previous investigations showing rapid dissolution of Mg-bearing phyllosilicates and slower dissolution of ferruginous phases during sulfuric acid leaching of laterites (Hariyanto et al., 2023; Shayakhmetova et al., 2025). Likewise, iron dissolution remained substantially lower than magnesium dissolution, in agreement with the behavior reported for limonitic laterites under atmospheric and pressure leaching conditions (He et al., 2022a; Çoban & Baş, 2024).

Figure 4 compares the extraction profiles of magnesium, nickel, and iron as a function of leaching time.

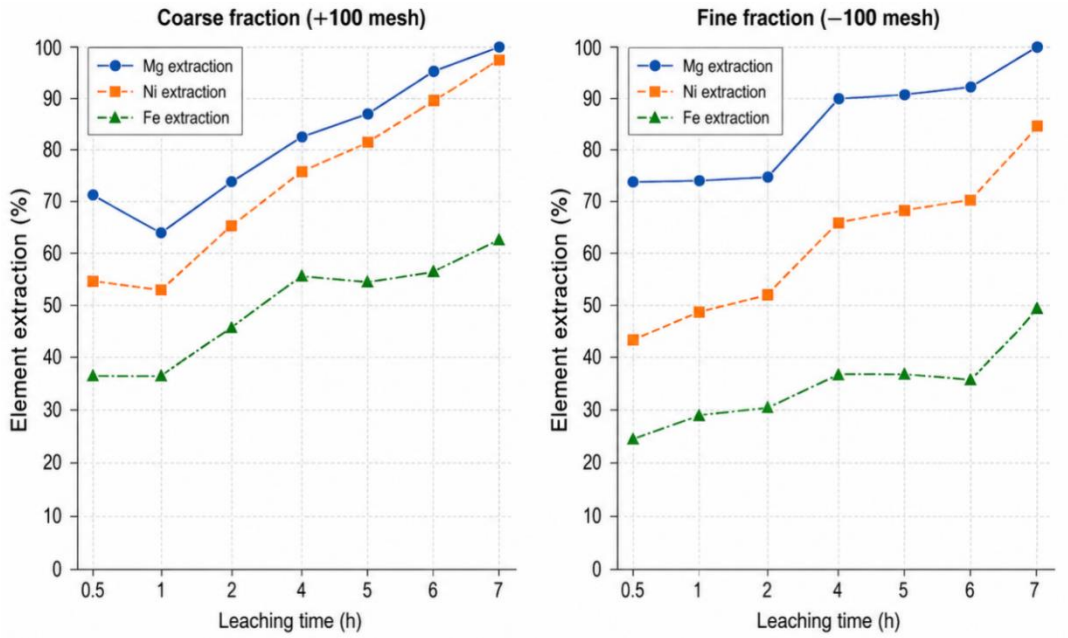

Figure 4. Dissolution behavior of Mg, Ni, and Fe during atmospheric sulfuric acid leaching.
Source: Authors.

The extraction sequence observed during leaching can be summarized as Mg > Ni > Fe, reflecting differences in the reactivity of mineral hosts and their dissolution mechanisms.

Kinetic Modeling

The experimental nickel extraction data were fitted with mechanistic and empirical kinetic models. The quality of each fit was evaluated using the coefficient of determination (R^2).

The performance of the evaluated kinetic models is presented in Table 6. The coefficient of determination (R^2) was used to compare the goodness of fit of each model for the coarse and fine fractions.

Table 5. Coefficients of determination (R^2) obtained for the kinetic models evaluated in this study.

Kinetic model	Linearized expression	R^2 Coarse fraction (>100#)	R^2 Fine fraction (<100#)
Pseudo-first-order	$-\ln(1 - X) = kt$	0.995	0.949
Pseudo-second-order	$t/X = 1/(kXe^2) + t/Xe$	0.999	0.990
SCM – Chemical reaction control	$1 - (1 - X)^{(1/3)} = kt$	0.978	0.974
SCM – Product layer diffusion control	$1 - 3(1 - X)^{(2/3)} + 2(1 - X) = kt$	0.987	0.972

Source: Authors.

Note: X represents fractional nickel extraction. R^2 values were calculated from the nickel extraction curves obtained for the coarse and fine fractions during atmospheric sulfuric acid leaching.

The pseudo-second-order model provided the best overall fit for the nickel extraction data in both particle-size fractions, with R^2 values of 0.999 for the coarse fraction and 0.990 for the fine fraction. The Shrinking Core Model also described the experimental data reasonably well, although with lower coefficients of determination. For the coarse fraction, the product-layer diffusion expression gave a slightly better fit than the chemical-reaction control model. In contrast, the fine fraction showed a marginally higher R^2 for the chemical reaction control expression. These differences indicate that

nickel dissolution cannot be described by a single rate-controlling mechanism across both fractions. Instead, the kinetic response appears to reflect the combined effect of rapid dissolution of readily leachable nickel-bearing phases and slower dissolution of more resistant mineral hosts.

The variation in model performance between the coarse and fine fractions supports the interpretation that particle-size-dependent mineralogical partitioning influenced the leaching mechanism. Similar mixed kinetic behavior has been reported in nickel laterite leaching studies applying Shrinking Core and pseudo-order models, where dissolution rates were affected by mineral host reactivity, particle texture, and diffusion limitations (Li et al., 2020; Garces-Granda et al., 2020; Borda & Torres, 2023; Alif et al., 2025; Tyassena et al., 2026).

Statistical assessment of extraction results

A descriptive statistical treatment was applied to the final magnesium-corrected extraction values obtained after 420 min of leaching. For each particle-size fraction, mean extraction, standard deviation (SD), and coefficient of variation (CV) were calculated from the four experimental tests. Because the tests were conducted with a fixed initial acid dosage, the calculated dispersion reflects the variability in the metallurgical response associated with particle-size fractions, mineralogical heterogeneity, and phase-specific dissolution behavior, rather than variability due to changes in acid addition. Therefore, the statistical parameters should be interpreted as indicators of response consistency under the evaluated leaching conditions, and not as measures of analytical repeatability alone. Table 7 summarizes a simplified comparison between the two alternatives.

Table 6. Statistical summary of final magnesium-corrected extraction values obtained for coarse and fine fractions.

Element	Coarse mean (%)	Coarse SD (%)	Coarse CV (%)	Fine mean (%)	Fine SD (%)	Fine CV (%)
Al	57.65	0.80	1.39	57.13	1.72	3.01
Co	65.70	5.62	8.55	64.65	6.30	9.74
Fe	57.28	5.81	10.15	55.95	6.17	11.03
Mg	100.00	0.00	0.00	100.00	0.00	0.00
Mn	46.90	4.26	9.08	45.73	5.03	11.00
Ni	93.38	6.08	6.51	92.00	5.82	6.33
Si	0.11	0.01	7.48	0.12	0.01	8.08

Source: Authors.

The final nickel extraction showed relatively low dispersion in both fractions, with CV values of 6.51% for the coarse fraction and 6.33% for the fine fraction. This indicates that high nickel recovery was consistently achieved under the fixed leaching conditions evaluated in this study. Cobalt, iron, and manganese exhibited higher coefficients of variation, reflecting their greater dependence on mineralogical associations, phase distributions, and selective dissolution behavior. Magnesium extraction was fixed at 100% after magnesium correction and was therefore not used as an independent indicator of experimental variability.

The statistical comparison indicates that the final nickel recoveries of the coarse and fine fractions were broadly similar, with mean values of 93.38% and 92.00%, respectively. The difference between the two means was only 1.38 percentage points, which is smaller than the observed standard deviation for both datasets. Therefore, the main distinction between the two fractions was not the ultimate nickel extraction, but the extraction rate and kinetic behavior during the first hours of leaching. This supports the interpretation that granulometric classification mainly affected the dissolution pathway and rate-controlling mechanisms rather than the final achievable nickel recovery.

Discussion

Why Does the Coarse Fraction Show Faster Initial Leaching?

The leaching behavior observed in this study was controlled by the combined effects of particle-size fraction and mineralogical composition. Therefore, differences in final extraction values should not be interpreted solely as a particle-size effect. Instead, the results represent the integrated metallurgical response of the coarse and fine fractions, reflecting their distinct mineralogical assemblages and nickel deportment characteristics.

Even considering this operational variation, the coarse fraction showed faster initial nickel extraction in the kinetic profiles. This behavior can be explained by its higher abundance of serpentine, vermiculite, chlorite, and poorly crystalline Fe–Si phases. These phases are more reactive under sulfuric acid leaching conditions than well-developed iron oxyhydroxides and can release nickel more rapidly during the early stages of leaching. Nickel hosted in Mg-bearing phyllosilicates is generally more accessible to acid attack than nickel structurally incorporated into goethitic phases. Similar relationships between phyllosilicate dissolution and nickel recovery have been reported for lateritic ores containing serpentine-rich or transitional mineral assemblages (Hariyanto et al., 2023; Jeong et al., 2025; Kang et al., 2026).

The rapid dissolution of magnesium supports this interpretation. Mg extraction reached high values early in the leaching tests and approached complete dissolution at the end of the experiments. This behavior indicates intense reaction of Mg-bearing phases, particularly serpentine and vermiculite-bearing particles. Since nickel was partly associated with these phases, their dissolution contributed to the rapid initial release of Ni in the coarse fraction.

The poorly crystalline Fe–Si phase also appears to have contributed to nickel release. This phase is texturally and chemically intermediate between silicate-rich and ferruginous domains and may behave as a more reactive nickel host than crystalline iron oxyhydroxides. Previous studies have shown that poorly crystalline or mixed Fe–Si lateritic phases may exert a strong influence on nickel deportment and metallurgical response, particularly in intensely weathered profiles with heterogeneous textures (Dybowska et al., 2022; Araujo et al., 2026). Thus, the faster initial response of the coarse fraction is best interpreted as the combined result of granulometric partitioning and mineralogical reactivity, rather than particle size alone.

Mineralogical and Kinetic Controls on Nickel Liberation

The results indicate that nickel liberation was controlled by both mineralogical host and acid availability. The coarse fraction contained higher proportions of serpentine, vermiculite–chlorite, and poorly crystalline Fe–Si phases. These phases promoted rapid Mg dissolution and faster early-stage Ni extraction. This sequence can be represented as:

Coarse fraction → higher phyllosilicate content → higher Mg dissolution → faster initial Ni release.

In contrast, the fine fraction was enriched in goethite–limonite. Nickel associated with iron oxyhydroxides is generally released through progressive dissolution of the ferruginous matrix, which proceeds more slowly under atmospheric sulfuric acid leaching conditions. This behavior can be represented as:

Fine fraction → higher goethite–limonite content → slower ferruginous matrix dissolution → slower Ni extraction kinetics.

The statistical comparison reinforces this point. The final mean nickel extraction values for the coarse and fine fractions were broadly similar, while their kinetic profiles differed more clearly during the early stages of leaching. This suggests that the main effect of particle-size-dependent mineralogy was not necessarily to change the ultimate achievable Ni recovery, but to modify the dissolution rate and the pathway by which nickel was released. Such behavior is consistent with geometallurgical concepts, in which metallurgical performance is controlled by mineral hosts, textures, liberation characteristics, and process conditions rather than by bulk chemical composition alone (Dehaine et al., 2021; Butcher et al., 2023). Similar mineralogical controls on nickel recovery have been reported for lateritic ores with variable nickel deportment among phyllosilicates, poorly crystalline Fe–Si phases, and iron oxyhydroxides (Araujo et al., 2026; Jeong et al., 2025).

The kinetic modeling provides additional insight. The pseudo-second-order model gave the best overall fit for both fractions, with R^2 values of 0.999 for the coarse fraction and 0.990 for the fine fraction. This indicates that nickel dissolution was influenced by the progressive availability of reactive sites and by the heterogeneous nature of the mineral assemblage. The pseudo-first-order model also fitted the coarse fraction well, but showed a weaker fit for the fine fraction, suggesting that the coarse material contained a larger proportion of readily leachable nickel-bearing phases.

The Shrinking Core Model results also support a mixed-mechanism interpretation. For the coarse fraction, the product layer diffusion expression showed a slightly better fit than the chemical reaction control model. This suggests that, after rapid initial dissolution of reactive phases, diffusion through altered particle surfaces or partially reacted layers may have contributed to the rate limitation. For the fine fraction, the chemical reaction control expression showed a marginally higher R^2 than the diffusion expression, indicating a stronger contribution from surface reaction processes associated with progressive dissolution of iron oxyhydroxides.

Overall, the kinetic results indicate that nickel dissolution was not governed by a single universal mechanism. Instead, the apparent controlling mechanism varied with mineralogical host and particle-size fraction. Similar mixed kinetic behavior has been reported in nickel laterite leaching studies using Shrinking Core and pseudo-order models, where dissolution rates were influenced by mineral host reactivity, particle texture, acid availability, and diffusion limitations (Li et al., 2020; Garces-Granda et al., 2020; Borda & Torres, 2023; Alif et al., 2025; Tyassena et al., 2026).

Geometallurgical Implications

The results demonstrate that granulometric classification can provide useful geometallurgical information for laterite processing. The coarse fraction was enriched in phyllosilicates and poorly crystalline Fe–Si phases and showed faster initial nickel dissolution. The fine fraction was enriched in goethite–limonite and exhibited a stronger association between nickel release and ferruginous matrix dissolution. These differences suggest that a single processing route may not be optimal for all particle-size fractions of a lateritic ore.

Based on the observed mineralogical partitioning, extraction behavior, and kinetic response, a particle-size-based processing strategy is proposed in Figure 5.

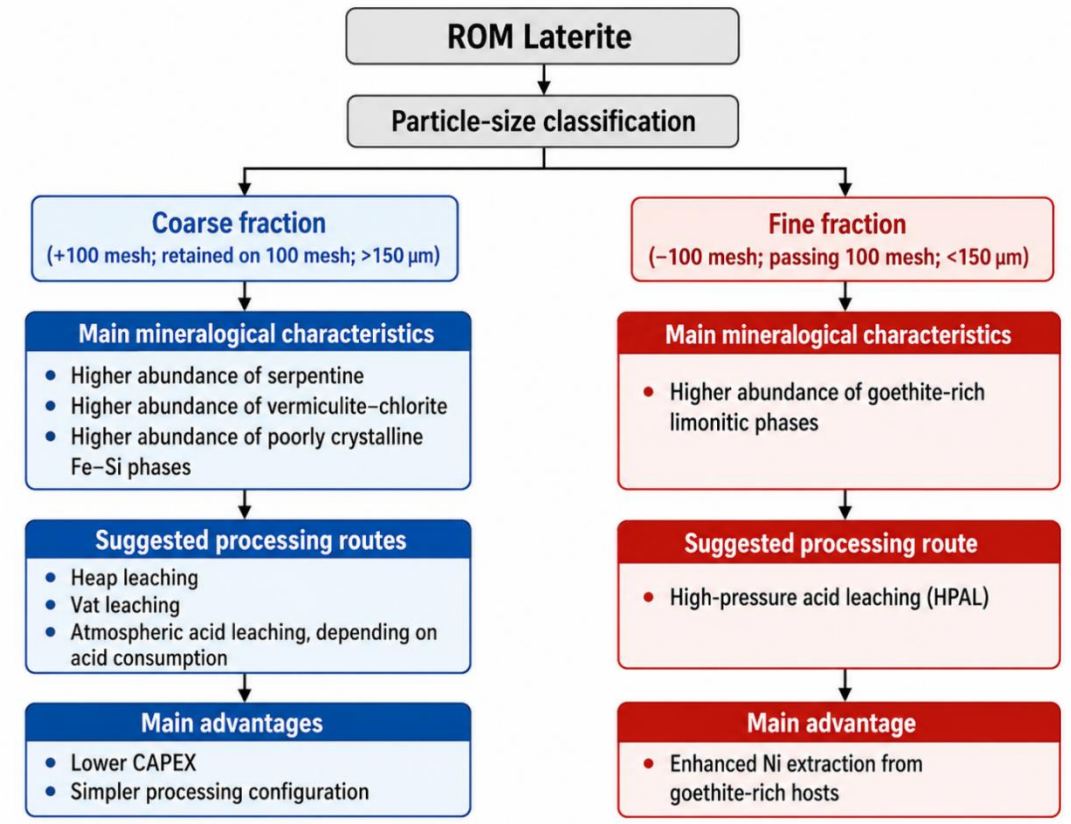

Figure 5. Conceptual geometallurgical flowsheet for particle-size-based processing of limonitic nickel laterite.
Source: Authors.

In the proposed flowsheet, run-of-mine laterite is first subjected to granulometric classification. The coarse fraction, enriched in serpentine, vermiculite–chlorite, and poorly crystalline Fe–Si phases, may be suitable for lower-CAPEX atmospheric leaching routes, including heap leaching, vat leaching, or atmospheric tank leaching. The faster initial kinetics observed for this fraction support its potential treatment under less severe pressure conditions. Atmospheric leaching routes have been successfully investigated for nickel laterites and may provide operational advantages when applied to suitable mineralogical domains (Prasetya et al., 2025; Ribeiro et al., 2025).

The fine fraction, enriched in goethite–limonite, may be more appropriate for high-pressure acid leaching. HPAL is particularly effective for limonitic laterites because it promotes extensive dissolution of nickel-bearing iron oxyhydroxides under elevated temperatures and pressures. Although HPAL involves higher capital intensity and more complex operations, it can achieve high recoveries of nickel and cobalt from fine ferruginous materials, where atmospheric leaching kinetics may be slower (Dickson et al., 2025; Bana et al., 2025; Surya et al., 2026).

This interpretation does not imply that coarse and fine fractions must always be processed separately. Rather, it shows that particle-size-dependent mineralogical information can support more flexible process design. A hybrid route could reduce the mass sent to HPAL by directing more reactive coarse material to atmospheric leaching, while reserving pressure leaching capacity for the fine limonitic fraction. This type of ore-domain-based routing is consistent with geometallurgical principles, in which mineralogical, textural, and metallurgical data are integrated to guide process selection and optimize value recovery (Dehaine et al., 2021; Butcher et al., 2023; Pell et al., 2021).

Although the present study did not separately calculate the actual sulfuric acid consumption for the coarse and fine fractions, the experimental design focused on evaluating the effects of particle size, mineralogical partitioning, and leaching kinetics on nickel extraction under fixed initial acid-dosage conditions.

Economic Assessment

A simplified economic assessment was developed to compare two conceptual processing alternatives for nickel laterite ores: (i) a single HPAL flowsheet, in which the full ROM laterite feed is directed to high-pressure acid leaching, and (ii) a hybrid flowsheet, in which particle-size classification is used to separate a coarse Mg-silicate-rich fraction from a fine goethite-rich limonitic fraction. In the hybrid concept, only the fine fraction is treated by HPAL, whereas the coarse fraction is directed to lower-pressure leaching routes such as heap leaching, vat leaching, or atmospheric acid leaching.

The assessment is intentionally preliminary and should be interpreted as a screening-level comparison rather than a definitive feasibility study. Nevertheless, it highlights the main economic drivers relevant in early project stages: HPAL

tonnage, sulfuric acid consumption, autoclave size, energy demand, materials of construction, residue neutralization, and operational complexity.

The main economic advantage of the hybrid configuration is the reduction of material reporting to HPAL. Since HPAL circuits require high-pressure autoclaves, titanium-lined equipment, high-temperature slurry handling, flash systems, steam generation, and robust acid-resistant materials, the capital cost is strongly influenced by the mass flow treated under pressure. Therefore, reducing the HPAL feed from 100% of the ROM to approximately 40–60% may significantly decrease the required autoclave volume, installed power, steam demand, and downstream pressure-leach infrastructure.

In addition, the hybrid route may potentially reduce acid consumption on a ROM basis, although this effect remains a screening-level hypothesis that must be validated through fraction-specific acid-consumption tests. This is particularly relevant when the coarse fraction contains higher proportions of serpentine, vermiculite–chlorite, and poorly crystalline Fe–Si phases, which may consume substantial acid without necessarily contributing proportionally to nickel recovery. By directing the goethite-rich fine fraction to HPAL, the process concentrates the high-pressure treatment on the fraction where nickel is more commonly associated with Fe oxyhydroxide phases and is more suitable for intensive acid leaching.

However, the hybrid route also introduces additional costs. These include particle-size classification, separate stockpiling or slurry handling of coarse and fine fractions, additional leaching equipment for the coarse stream, more complex process control, and possibly longer residence times for atmospheric or heap/vat leaching. Therefore, the economic benefit depends on whether the reduction in HPAL CAPEX and OPEX outweighs the extra cost of the parallel coarse-fraction treatment circuit.

Table 8 summarizes a simplified comparison between the two alternatives.

Table 7. Simplified economic comparison between single HPAL and hybrid laterite processing routes

Item	Single HPAL process	Hybrid process
HPAL tonnage	100% of ROM feed	40–60% of ROM feed
Acid consumption	High; typically controlled by the full mineralogical variability of the ROM, including Mg-silicate acid consumers	Moderate to high; reduced on a ROM basis because HPAL is focused on the fine goethite-rich fraction, while coarse material may be treated under less intensive conditions
CAPEX	Very high; large autoclave capacity, high-pressure slurry handling, titanium-lined equipment, steam generation, flash cooling, and neutralization systems	Moderate to high; smaller HPAL circuit, but additional cost for classification, coarse-fraction leaching, material handling, and split-stream control
OPEX	High; acid, steam, oxygen/oxidant if required, neutralizing reagent, maintenance, scaling control, and residue management	Potentially lower; reduced HPAL acid and energy demand, but partly offset by coarse-fraction leaching cost, longer residence time, solution management, and additional operational complexity
Main economic advantage	Simpler flowsheet integration and single leaching route	Reduced HPAL duty and improved allocation of intensive processing to the most suitable mineralogical fraction
Main economic risk	Overdesign of HPAL circuit if part of the feed has low nickel response or high acid consumption	Economic penalty if coarse-fraction recovery is low or if classification does not produce strong mineralogical upgrading
Relative CAPEX index	1.00	0.65–0.85
Relative OPEX index	1.00	0.70–0.90
Preferred condition	Homogeneous limonitic feed with high HPAL response	Heterogeneous laterite feed with clear mineralogical separation between coarse Mg-silicate-rich and fine goethite-rich fractions

Source: Author's conceptual estimate based on simplified flowsheet comparison; values are indicative and should be validated by pilot testing, mass balance, acid consumption tests, and project-specific CAPEX/OPEX estimation.

From an economic perspective, the hybrid flowsheet is most attractive when particle-size classification produces a meaningful separation between mineralogical domains. If the fine fraction contains most of the goethite-hosted nickel and accounts for only 40–60% of the ROM mass, the HPAL circuit can be designed for a substantially lower throughput. This reduction directly affects autoclave volume, installed pressure equipment, steam generation, and downstream neutralization capacity.

A simplified normalized cost relationship may be expressed as:

$$C_{HPAL,h} = C_{HPAL,s} \times f_{HPAL}^{n}$$

where $C_{HPAL,h}$is the estimated HPAL capital cost in the hybrid route, $C_{HPAL,s}$is the HPAL capital cost in the single-route flowsheet, $f_{HPAL}$is the fraction of ROM treated by HPAL, and $n$is a scaling exponent. For preliminary screening, $n$may be assumed to be between 0.6 and 0.8. Thus, if only 50% of the ROM is treated by HPAL, the HPAL-related capital cost may decrease substantially, although not linearly, because some fixed infrastructure remains necessary (Peters et al., 2003; Towler & Sinnott, 2013; Turton et al., 2018).

The acid cost can also be expressed on a ROM basis:

$$AC_{ROM} = A_f \times f_f + A_c \times f_c$$

where $AC_{ROM}$is the total acid consumption per tonne of ROM, $A_f$is the acid consumption of the fine fraction, $f_f$is the mass fraction of fines, $A_c$is the acid consumption of the coarse fraction, and $f_c$is the mass fraction of coarse material. This equation highlights that the hybrid route is economically favorable only if the coarse-fraction leaching route can achieve acceptable nickel recovery at lower acid intensity than HPAL treatment of the full ROM feed (Çoban & Baş, 2024; Dickson et al., 2025; Araujo et al., 2026; Astuti et al., 2024).

The hybrid process offers more targeted processing by applying HPAL to the most responsive ore fraction and treating the coarse fraction with lower-cost methods. This can improve project economics, especially in heterogeneous laterite deposits with variable mineralogy, nickel deportment, and acid use. However, final viability requires tests like locked-cycle leaching, residue analysis, nickel recovery modeling, and cash flow analysis.

Conclusions

This study demonstrated that particle-size classification is not only a physical separation step, but also a useful geometallurgical tool for interpreting the processing behavior of nickel laterites. The results indicate that nickel-bearing minerals were unevenly distributed between the coarse and fine fractions, leading to distinct mineralogical assemblages and different leaching responses under atmospheric sulfuric acid leaching conditions.

The coarse fraction was characterized by higher proportions of serpentine, vermiculite–chlorite, and poorly crystalline Fe–Si phases. These phases are interpreted as important nickel-bearing hosts and contributed to a faster initial leaching response compared with the fine fraction. This behavior suggests that part of the nickel associated with phyllosilicates and mixed Fe–Si phases may be more readily accessible under atmospheric acid leaching conditions, depending on acid consumption, mineral exposure, and mineralogical variability.

In contrast, the fine fraction was dominated by goethite-rich limonitic phases, indicating a stronger association of nickel with iron oxyhydroxide minerals. This mineralogical signature is consistent with the behavior expected for limonitic laterites and helps explain the slower approach to high nickel extraction observed for the fine fraction. Although both fractions reached high final nickel recovery after prolonged leaching, their kinetic responses were different, showing that particle-size-dependent mineralogy affected mainly the dissolution rate and residence-time requirement rather than the final achievable nickel extraction.

The findings support the evaluation of a hybrid processing strategy, in which particle-size classification is used to guide route selection for different ore fractions. In this conceptual approach, the fine goethite-rich fraction may be considered for high-pressure acid leaching (HPAL), whereas the coarse phyllosilicate-rich fraction may be evaluated for heap leaching, vat leaching, or atmospheric acid leaching. Such selective routing may have the potential to reduce the tonnage reporting to HPAL, decrease autoclave duty, lower energy demand, and improve process flexibility. However, these potential benefits should be validated through fraction-specific acid-consumption tests, mass-balance studies, and techno-economic assessment.

Overall, the study highlights the importance of integrating particle-size analysis, automated mineralogy, nickel deportment, and leaching kinetics into early-stage process design. For heterogeneous laterite deposits, granulometric classification can provide a practical basis for geometallurgical domaining and flowsheet optimization. Future work should include locked-cycle leaching tests, detailed acid-consumption balances, residue characterization, pilot-scale classification trials, and techno-economic evaluation to confirm the industrial applicability of the proposed hybrid route.

References

1. Abdollahi, H., Hosseini-Nasab, M., & Yadollahi, A. (2024). Bioleaching of lateritic nickel ores. In M. S. Hesami, A. Mousavi Khaneghah, & M. Soltani (Eds.), *Biotechnological innovations in the mineral-metal industry* (pp. 41–66). Springer Nature. https://doi.org/10.1007/978-3-031-43625-3_3.
2. Acquah, G., Abaka-Wood, G., Skinner, W., Addai-Mensah, J., & Asamoah, R. (2025). Effect of mechanical activation on nickel and cobalt extraction in refractory nickel laterite ore. Powder Technology, 468, 121655. https://doi.org/10.1016/j.powtec.2025.121655.
3. Acquah, G., Skinner, W., Abaka-Wood, G., Spiridonov, P., Addai-Mensah, J., & Asamoah, R. (2026). Extraction of nickel and cobalt from complex low-grade lateritic ores: Challenges and opportunities.

Minerals, 16(3), Article 287. https://doi.org/10.3390/min16030287.

4. Alif, M. N., Kim, S., Tomas Da Rocha, L., & Jung, S.-M. (2025). Phosphoric acid leaching of laterite ore: Mechanism and kinetics analysis of Ni and Co extraction. *Metallurgical and Materials Transactions B, 56*(3), 3140–3151. https://doi.org/10.1007/s11663-025-03527-6.
5. Araujo, F. P., Magalhães, N., Vassilieva, E., Rollinson, G., Andersen, J. C. Ø., Crane, R., Tampouris, S., Hughes, H. S. R., & Muchez, P. (2026). Mineralogical controls on Ni and Co recovery during HCl leaching of laterites. *International Journal of Minerals, Metallurgy and Materials, 33*(6). https://doi.org/10.1007/s12613-026-3396-7
6. Astuti, W., Avista, D., Prihutami, P., Wanta, K. C., Prakosa, A., Anggara, F., & Petrus, H. T. B. M. (2024). Atmospheric leaching behavior and kinetics of nickel and cobalt from Halmahera limonite ore. *International Journal of Technology*, *15*(4), 824–833. https://doi.org/10.14716/ijtech.v15i4.5607.
7. Bana, I. S., Wan, W., & Shen, L. (2025). Optimization of high-pressure acid leaching for nickel and cobalt recovery from ultralow-grade laterite ores. *JOM, 77*(7), 5192–5204. https://doi.org/10.1007/s11837-025-07402-2.
8. Borda, J., & Torres, R. (2023). Effect of pretreatments to improve nickel leaching from laterites in carboxylic media: Mechanism and kinetic model. *South African Journal of Chemical Engineering, 46*(3). https://doi.org/10.1016/j.sajce.2023.07.001.
9. Butcher, A. R., Dehaine, Q., Menzies, A. H., & Michaux, S. P. (2023). Characterisation of ore properties for geometallurgy. *Elements, 19*(6), 352–358. https://doi.org/10.2138/gselements.19.6.352.
10. Cao, S., Chang, L., Bi, X., & Luo, S. (2022). Alkaline hydrothermal treatment and leaching kinetics of silicon from laterite nickel ore. *Mining, Metallurgy & Exploration, 39*(4). https://doi.org/10.1007/s42461-021-00518-4.
11. Çetintaş, S., & Bingöl, D. (2020). Performance evaluation of leaching processes with and without ultrasound effect combined with reagent-assisted mechanochemical process for nickel recovery from Laterite: Process optimization and kinetic evaluation. *Minerals Engineering*, *157*, 106562.
12. Çoban, B., & Baş, A. D. (2024). HPAL of a lateritic nickel ore: An investigation on the relationship between nickel and cobalt extraction and acid consumption. *Minerals Engineering, 218*, Article 109014. https://doi.org/10.1016/j.mineng.2024.109014.
13. Dehaine, Q., Tijsseling, L. T., Glass, H. J., Törmänen, T., & Butcher, A. R. (2021). Geometallurgy of cobalt ores: A review. *Minerals Engineering, 160*, Article 106656. https://doi.org/10.1016/j.mineng.2020.106656
14. Dickson, O. V., Deleau, T., Espitalier, F., Coquelet, C., Lombart, J., & Accart, P. (2025). High-pressure acid leaching of laterite ores: Effect of acid and solid content on Ni and Co yield under non-isothermal and isothermal conditions. *Hydrometallurgy, 238*, Article 106576. https://doi.org/10.1016/j.hydromet.2025.106576
15. Domènech, C., Villanova-de-Benavent, C., Proenza, J. A., Tauler, E., Lara, L., Galí, S., Soler, J. M., Campeny, M., & Ibañez-Insa, J. (2022). Co–Mn mineralisations in the Ni laterite deposits of Loma Caribe (Dominican Republic) and Loma de Hierro (Venezuela). *Minerals, 12*(8), Article 927. https://doi.org/10.3390/min12080927.
16. Dybowska, A., Schofield, P. F., Newsome, L., Herrington, R. J., Mosselmans, J. F. W., Kaulich, B., Kazemian, M., Araki, T., Skiggs, T. J., Kruger, J., Oxley, A., Norman, R. L., & Lloyd, J. R. (2022). Evolution of the Piauí laterite, Brazil: Mineralogical, geochemical and geomicrobiological mechanisms for cobalt and nickel enrichment. *Minerals, 12*(10), Article 1298. https://doi.org/10.3390/min12101298.
17. Garces-Granda, A., Lapidus, G. T., & Restrepo-Baena, O. J. (2020). Effect of a thermal pretreatment on dissolution kinetics of a limonitic laterite ore in chloride media. *Hydrometallurgy, 196*, Article 105428. https://doi.org/10.1016/j.hydromet.2020.105428.
18. Gharaei, A. A., Rezai, B., & Hamidian-Shormasti, H. (2024). Environmental friendly approach: Atmospheric and high-pressure acid leaching studies, low-grade laterites nickel processing. Journal of Mining and Environment, 15(4), 1591–1606. https://doi.org/10.22044/jme.2024.14230.2656
19. Golroudbary, S. R, Kraslawski, A., Wilson, B. P., & Lundström, M. (2023). Assessment of environmental sustainability of nickel required for mobility transition. *Frontiers in Chemical Engineering*, *4*, Article 978842. https://doi.org/10.3389/fceng.2022.978842
20. Hariyanto, R. K. S., Tomas Da Rocha, L., Kim, S.-J., & Jung, S.-M. (2023). Extraction behavior of nickel and cobalt from serpentine-rich ore through sulfation-roasting-leaching process. *Metallurgical and Materials Transactions B, 54*(6), 2915–2928. https://doi.org/10.1007/s11663-023-02934-x.
21. He, F., Ma, B., Wang, C., & Chen, Y. (2022). Mineral evolution and porous kinetics of nitric acid pressure leaching limonitic laterite. *Minerals Engineering, 181*, Article 107544. https://doi.org/10.1016/j.mineng.2022.107544.
22. He, F., Ma, B., Wang, C., Zuo, Y., & Chen, Y. (2022). Dissolution behavior and porous kinetics of limonitic laterite during nitric acid atmospheric leaching. *Minerals Engineering, 185*, Article 107671. https://doi.org/10.1016/j.mineng.2022.107671.

23. Jeong, H.-E., Kang, H., Choi, S., & Kim, H. (2025). Comparative study of limonitic and saprolitic laterite ores on the leaching characteristics under atmospheric pressure. *Minerals Engineering, 226*, Article 109250. https://doi.org/10.1016/j.mineng.2025.109250.
24. Kang, H., Kim, J., & Kim, H.-J. (2026). Early-stage temperature-dependent leaching kinetics and mechanisms of saprolitic and limonitic nickel laterite ores under atmospheric conditions. *Minerals Engineering*, Article 110115. https://doi.org/10.1016/j.mineng.2026.110115.
25. Komnitsas, K., Karmali, V., Bartzas, G., & Kritikaki, A. (2026). Hydrochloric acid leaching of low-grade limonitic laterite. *Circular Economy and Sustainability*, *6*(2), Article 119. https://doi.org/10.1007/s43615-026-00886-3.
26. Li, G., Chen, Y., Mang, C., Teng, X., Luo, J., & Rao, M. (2023). Near-zero-waste approach for the treatment of saprolitic nickel laterite via a combined hydrometallurgical process. *ACS Sustainable Chemistry & Engineering, 11*(18). https://doi.org/10.1021/acssuschemeng.2c05403.
27. Li, J., Yang, Y., Wen, Y., Liu, W., Chu, Y., Wang, R., & Xu, Z. (2020). Leaching kinetics and mechanism of laterite with NH4Cl-HCl solution. *Minerals, 10*(9), Article 754. https://doi.org/10.3390/min10090754.
28. Li, J., Yu, T., Li, C., Han, X., & Gao, J. (2025). Efficient and selective leaching of nickel and cobalt from nickel laterite ore by a combined atmospheric acid leaching-ferric chloride solution leaching process: Optimization and mechanism. *RSC Advances, 15*(36), 29176–29189. https://doi.org/10.1039/D5RA04469C.
29. Nasab, M. H., Noaparast, M., & Abdollahi, H. (2020). Dissolution of nickel and cobalt from iron-rich laterite ores using different organic acids. *Journal of Mining and Environment, 11*(3), 779–797. https://doi.org/10.22044/jme.2020.9564.1869.
30. Ni'mah, Y. L., Hernanda, R. A., & Suprapto, S. (2026). Nickel extraction from Kolaka laterite ore: A HCl leaching optimization method using the BBD-RSM and recovery via oxalate precipitation. *Engineering, Technology & Applied Science Research, 16*(1), 31795–31801. https://doi.org/10.48084/etasr.15251.
31. Osali, M., Ahani, F., Aboutalebi, M. R., Adeli, M., Moghaddam, J., Karimi, S., Wijenayake, J. J., & Alagha, L. (2026). Selective extraction of nickel and cobalt from limonitic laterite via optimized sulfation roasting–water leaching and solvent extraction. *Minerals, 16*(5), Article 431. https://doi.org/10.3390/min16050431.
32. Pell, R., Tijsseling, L., Goodenough, K., Wall, F., Dehaine, Q., Grant, A., Deak, D., Yan, X., & Whattoff, P. (2021). Towards sustainable extraction of technology materials through integrated approaches. *Nature Reviews Earth & Environment, 2*, 665–679. https://doi.org/10.1038/s43017-021-00211-6.
33. Pereira, A. C., dos Santos, J. R., & Fonseca, R. B. da C. (2025). Determination of free acidity in sulfuric liquors using the oxalate method: Scope, limitations, and validation. REMUNOM, 18(2). https://doi.org/10.61164/1knf6e79
34. Pereira, A. C. (2026). Controlling co-precipitation in hydrometallurgy: From physicochemical parameters to process design and technology readiness. IKR Journal of Engineering and Technology, 2(3). https://doi.org/10.5281/zenodo.20357561
35. Pereira, A. C. (2026). Free acidity in hydrometallurgy is not pH: A critical review of measurement methods, errors, and process consequences. International Journal of Current Science Research and Review, 9(3), 1233–1260. https://doi.org/10.47191/IJCSRR/V9-i3-14
36. Peters, M. S., Timmerhaus, K. D., & West, R. E. (2004). *Plant design and economics for chemical engineers* (5th ed.). McGraw-Hill..
37. Prameswara, G., Amin, I., Ulfah, A. N., Trisnawati, I., Petrus, H. T. B. M., & Puspita, F. (2024). Atmospheric leaching behavior and kinetics study of roasted laterite ore. *Mining, Metallurgy & Exploration, 41*, 1025–1033. https://doi.org/10.1007/s42461-024-00947-x.
38. Prasetya, A., Putera, A. D. P., Sujoto, V. S. H., Zaidan, M. H., Abdurrahman, M. T., Andriani, A., Astuti, W., Sutijan, & Petrus, H. T. B. M. (2025). Enhanced recovery of nickel and cobalt from limonitic laterite ore: Optimization and kinetics of atmospheric sulfuric acid leaching. *Journal of Sustainable Metallurgy, 11*(4), 4127–4140. https://doi.org/10.1007/s40831-025-01231-y.
39. Ribeiro, G. da S., Nascimento, N. de D., Ribeiro, R. da S., Miranda, M. de P. M., Martins, P. R., Caetano, G. C., Andrade, L. A. de, & Ostroski, I. C. (2025). Optimization of the atmospheric acid leaching process for the recovery of nickel and cobalt from iron-rich lateritic ore. *Mining, Metallurgy & Exploration, 42*, 1127–1140. https://doi.org/10.1007/s42461-025-01233-0.
40. Ribeiro, P. P. M., dos Santos, I. D., Neumann, R., Fernandes, A., & Dutra, A. J. B. (2021). Roasting and leaching behavior of nickel laterite ore. *Metallurgical and Materials Transactions B, 52*(3), 1739–1754. https://doi.org/10.1007/s11663-021-02141-6.
41. Ribeiro, P. P. M., Neumann, R., Santos, I. D., & Dutra, A. J. B. (2022). An alternative route to extract nickel and cobalt from non-commercial laterite ore. *REM: International Engineering Journal, 75*(3), 245–257. https://doi.org/10.1590/0370-44672021750048.
42. Santos, A. L. A., Becheleni, E. M. A., Viana, P. R. M., Papini, R. M., et al. (2021). Kinetics of atmospheric leaching from a Brazilian nickel laterite ore allied to redox potential control. *Mining, Metallurgy &*

Exploration, 38, 187–201. https://doi.org/10.1007/s42461-020-00310-w.

43. Shayakhmetova, R., Mukhametzhanova, A., Osipov, P., Kali, A., Kuandykova, A., & Rakhym, A. (2025). Mechanism, kinetics and thermodynamics of nickel, iron, and magnesium hydrochloric acid leaching from laterite ore. *Scientific Reports, 15*, Article 41342. https://doi.org/10.1038/s41598-025-25276-x
44. Soh Tamehe, L., Zhao, Y., Xu, W., & Gao, J. (2024). Ni(Co) laterite deposits of Southeast Asia: A review and perspective. *Minerals, 14*(2), Article 134. https://doi.org/10.3390/min14020134.
45. Souza, R. F. M., Tavares, M. A. A., Cruz, L. E. C., Oliveira, V. A. A., Santos, I. D., Moura, F. J., & Brocchi, E. A. (2022). On the cobalt content upgrade in nickeliferous laterites using iron(III) sulfate: A study based on thermodynamics simulations. *Minerals, 12*(9), Article 1156. https://doi.org/10.3390/min12091156.
46. Surya, B. P., Liu, W., Yan, X., Xu, K., Wang, Q., Zhao, F., & Chai, L. (2026). Enhancing nickel recovery from laterite ores via high-pressure acid leaching: Machine learning and design of experiments for process optimization and environmental sustainability. *Journal of Sustainable Metallurgy, 12*(1), 122–141. https://doi.org/10.1007/s40831-025-01290-1.
47. Top, S., Kursunoglu, S., & Ichlas, Z. T. (2020). Effects of leaching parameters on the dissolution of nickel, cobalt, manganese and iron from Caldag lateritic nickel ore in hydrochloric acid solution. *Canadian Metallurgical Quarterly, 59*(3), 368–376. https://doi.org/10.1080/00084433.2020.1780560.
48. Towler, G., & Sinnott, R. K. (2013). *Chemical engineering design: Principles, practice and economics of plant and process design* (2nd ed.). Elsevier
49. Tunç Parlak, T., & Yildiz, K. (2025). Investigation of the effect of mechanical activation on nickel and cobalt extraction from laterite at atmospheric pressure by kinetics and leach residue analysis. *Canadian Metallurgical Quarterly, 64*(2), 680–697. https://doi.org/10.1080/00084433.2024.2366717
50. Turton, R., Shaeiwitz, J. A., Bhattacharyya, D., & Whiting, W. B. (2018). *Analysis, synthesis, and design of chemical processes* (5th ed.). Prentice Hall.
51. Tyassena, F. Y. P., Zuhud AL, M. D., Abrilla, A. M. A., Sarwana, W., Setyorini, D., Syafaatullah, A. Q., Ganing, M., Arninda, A., Rahim, H., & Prameswara, G. (2026). Optimizing microwave-assisted leaching of nickel from laterite ores: RSM-based modelling and kinetics. *Chemical Papers*. https://doi.org/10.1007/s11696-026-04911-5
52. Yunita, F. E., & Mubarok, M. Z. (2021). Nickel leaching from laterite ores by combination of organic and sulfuric acid. *AIP Conference Proceedings, 2382*(1), Article 050003. https://doi.org/10.1063/5.0060750.
53. Zhao, Z., Li, H., Wang, C., & Xing, P. (2025). Selective and efficient extraction of nickel and cobalt from laterite ores using the sulfation-roasting and leaching-precipitation process with H2O2 and surfactant addition. *Hydrometallurgy, 237*, 106546. https://doi.org/10.1016/j.hydromet.2025.106546.